

Demodulation performance of Galileo E1 OS and GPS L1C messages in a mobile environment

Axel Javier Garcia Peña, Marie-Laure Boucheret, Christophe Macabiau, Anne-Christine Escher, Lionel Ries

▶ **To cite this version:**

Axel Javier Garcia Peña, Marie-Laure Boucheret, Christophe Macabiau, Anne-Christine Escher, Lionel Ries. Demodulation performance of Galileo E1 OS and GPS L1C messages in a mobile environment. GNSS 2009, 22nd International Technical Meeting of The Satellite Division of the Institute of Navigation, Sep 2009, Savannah, United States. pp 2875 - 2889. hal-01022158

HAL Id: hal-01022158
https://enac.hal.science/hal-01022158

Submitted on 30 Sep 2014

HAL is a multi-disciplinary open access archive for the deposit and dissemination of scientific research documents, whether they are published or not. The documents may come from teaching and research institutions in France or abroad, or from public or private research centers.

L'archive ouverte pluridisciplinaire **HAL**, est destinée au dépôt et à la diffusion de documents scientifiques de niveau recherche, publiés ou non, émanant des établissements d'enseignement et de recherche français ou étrangers, des laboratoires publics ou privés.

Demodulation Performance of Galileo E1 OS and GPS L1C Messages in a Mobile Environment

Axel Garcia Pena, *Centre Nationale d'Etudes Spatiales (CNES)/TeSA*
Marie-Laure Boucheret, *IRIT, Université de Toulouse/ENSEEIHT*
Christophe Macabiau, *Ecole Nationale de l'Aviation Civile*
Anne-Christine Escher, *Ecole Nationale de l'Aviation Civile*
Lionel Ries, *Centre National d'Etudes Spatiales*

BIOGRAPHY

Axel Garcia Peña is a telecommunication engineer. He followed a European program of double degree: he graduated in 2006 from SUPAERO (Ecole Nationale Superieure de l'Aeronautique et de l'Espace) in Toulouse, France and he also obtained the engineer degree from ETSETB-UPC (Escola Tecnica Superior d'Enginyeria de Telecomunicacions de Barcelona – Universitat Politecnica de Catalunya, Spain) in 2006. He is now a PhD Student at ENAC and studies improved methods/algorithms to better demodulate the GPS signals as well as future navigation message structures.

Marie-Laure Boucheret graduated from the ENST Bretagne in 1985 (Engineering degree in Electrical Engineering) and from Telecom Paris in 1997 (PhD degree). She worked as an engineer in Alcatel Space from 1986 to 1991 then moved to ENST as an Associated Professor then a Professor. Currently, she is a Professor at ENSEEIHT. Her fields of interest are digital communications (modulation/coding, digital receivers, multicarrier communications…), satellite onboard processing (filter banks, DBFN…) and navigation system.

Christophe Macabiau graduated as an electronics engineer in 1992 from ENAC in Toulouse, France. Since 1994, he has been working on the application of satellite navigation techniques to civil aviation. He received his PhD in 1997 and has been in charge of the signal processing lab of the ENAC since 2000.

Anne-Christine Escher graduated as an electronics engineer in 1999 from the ENAC in Toulouse, France. Since 2002, she has been working as an associate researcher in the signal processing lab of the ENAC. She received her Ph.D. in 2003.

Lionel Ries is head of the Signal and RadioNavigation department of the CNES Radiofrequency sub-directorate since august 2009. He was a navigation engineer in the Transmission Techniques and signal processing department, at CNES since June 2000, responsible for research activities on GNSS2 signals.

ABSTRACT

The demodulation performance of the different GNSS signals, GPS L1C and GALILEO E1 OS, has already been analyzed in open environments. This type of environment is characterized by a permanent availability of a direct line of sight (LOS) satellite signal and weak multipath power relative to the LOS signal power. However, nowadays, there is an increasing demand for positioning services in urban environments, where the satellite signal propagation channel is significantly different from the Gaussian channel and thus the received signal may be notably affected.

The main differences between these 2 environments are the diminution of the direct signal power due to shadowing and/or obstacles blockage effect, and the strong presence of multipath in relation to the LOS signal power. Consequently, the received signal is the sum of the direct LOS signal and the multipath component, and this results into an equivalent received signal with a power and a phase changing constantly.

The aim of this paper is thus to analyze the demodulation performance of the GPS L1C and GALILEO E1 OS signals when they are transmitted through a mobile channel. More exactly, this paper studies the level of Bit Error Rate (BER), of Word Error Rate (WER) and of Ephemeris Error rate (EER) with respect to the C/N0 for each of the previously defined GNSS signals.

The mobile channel is modeled as a channel providing a received signal following a Loo distribution [12]. Three different phase tracking methods are analyzed: a PLL, an ideal phase estimation from an ideal channel estimation and a phase estimation obtained from a real channel estimation.

I. INTRODUCTION

The study presented in this paper is part of a Ph. D. thesis whose main objective is the optimization of the demodulation performance of the GNSS navigation message ephemeris data. One of the basic steps of this Ph. D. thesis is the analysis of the current performance of two of these new GNSS signals, GPS L1C and GALILEO E1 OS. This analysis was done from the current public available signal documents: GALILEO E1 OS ICD Draft 1 [2] and IS-GPS-800 [1].

Several studies of the performance of the current or future GNSS signals, GPS L1 C/A, GPS L2C, GPS L5, GPS L1C and GALILEO E1 OS have been realized over the years [3][13][14][15]. Almost all these studies have in common the assumption of an AWGN channel as a model for the transmission channel. This choice was completely justified because the main environments where the satellite positioning process was applied were open environments. These kinds of environments are mainly characterized by the constant availability line-of-sight (LOS) satellite signal, and by a negligible multipath power relative to the LOS signal power. Therefore, the received signal can be simply modeled as a signal with a constant power determined by the satellite-receiver distance and the only noise taken into account is the thermal noise which is generally modeled as an AWGN.

However, the growth of popularity of the positioning services has made these traditional open environments change. Nowadays, the majority of applications are vehicular or pedestrian applications in villages, cities and even indoor buildings. All these new scenarios have several characteristics in common and thus can be represented with the same mathematical model representing the transmission channel: all of them are referred as mobile environments/channels.

The main characteristics of these environments are the following: the LOS signal is quite attenuated and varies significantly in time, and the presence of multipath is strong and can no longer be neglected in relation to the LOS signal power. Therefore, the received signal is the addition of the attenuated LOS signal plus the multipath, which results into an equivalent signal with a power and a phase constantly changing, because the addition of the multipath on the LOS signal can be a constructive or destructive effect.

Nevertheless, these scenarios have already been analyzed in the terrestrial and satellite communications frame. Therefore, this paper reuses the most adapted mathematical model among the different mathematical models proposed for the analysis of satellite communication. More specifically, this paper has chosen the model presented by Perez-Fontan et al. [9][10], which is mainly a three-state model representing the high dynamic range of the received satellite power, whose transitions states are controlled by a first-order Markov chain and the state frame length. Finally, the equivalent received signal amplitude and phase are modeled with a Loo distribution whose parameters depend exclusively on the current model state among the 3 possible states. Nevertheless, this paper only analyses the performance in the LOS conditions state. The justification and the details of the model are presented in the next section.

In addition to changing the transmission channel model, another important variation taken into account is the carrier tracking techniques. In an AWGN channel, the phase is supposed constant or having small and slow variations, whereas in a mobile channel the phase, as well as the power, change more quickly. Therefore, the phase tracking performance is much more important in this latter case and it influences a lot more the demodulation performance. Thus, it is interesting to explore new forms of tracking the signal phase such as the phase estimation of the pilot channel. This means that this paper analyzes the demodulation performance of the different GNSS signals using three different types of phase tracking: the traditional PLL, the ideal phase estimation of the pilot channel and a first proposed estimation of the pilot channel.

Moreover, the phase and power variations of the received signal depend on the speed at which the receiver moves. In fact, the speed determines the time needed by the receiver to cover a state frame length and the variations of the multipath. And these variations of the multipath component are responsible for modifying the phase and power of the equivalent signal. In this paper, the case where a car travels at velocity of 30 km/h has been analyzed.

Finally, this paper not only presents the BER, Bit Error Rate, of the GPS L1C and GALILEO E1 OS signals, but also shows the WER, Word Error Rate, and EER, Ephemeris Error Rate since these two last figures of merit, mainly the latter one, are the most important values for a user. The reason is that they give the percentage of time where a receiver is capable of recovering the satellite position and the clock parameters, which is the only required transmitted information to obtain its own position.

This paper first gives a brief description of the two studied GNSS signals and continues by presenting the mobile channel and justifying the chosen mathematical model. Third, it defines the different phase tracking methods analyzed and follows with the justification of the assumptions of the study. Fifth, the paper describes the scenario or case used in the simulations and continues by presenting the results of the comparison between the demodulation performance of the different phase tracking methods and between the demodulation performance of the two GNSS signals. Finally, the paper summarizes the conclusions extracted from the previous results.

II. MAIN SIGNAL CHARACTERISTICS

The main characteristics of the GPS L1C and GALILEO E1 OS signals which condition the demodulation performance analyzed in this paper are the signal channel relative power distribution, the symbol transmission rate and the data message structure.

A. Signal Channel Relative Power Distribution:

Both signals, GPS L1C and GALILEO E1 OS, are received with the same level of power at the receiver antenna output. However, they distribute this power differently between the different channels forming them. Therefore, since the data channel and the pilot (dataless) channel are uncorrelated, the total received power can be expressed as:

Total signal power = Data signal power + Pilot signal power

The power distribution over each channel is the following:

Signal	***Data Channel***	***Pilot Channel***
GPS L1C	25%	75%
GALILEO E1 OS	50%	50%

Table 1: Signal Channel Relative Power Distribution between the data and pilot channels of the GPS L1C and GALILEO E1 OS signals

B. Symbol Transmission Rate (R_D):

The symbol transmission rate is 2.5 times higher for the European signal:

Signal	GPS L1C	GALILEO E1 OS
Symbol Tx Rate (R_D)	100 symb/s	250 symb/s

Table 2: Symbol Transmission Rate for GPS L1C and GALILEO E1 OS

C. Data Message Structure:

The data message structure is completely different for GPS L1C and GALILEO E1 OS. In fact, both the size and frequency of the information units (word, subframe, frame…) and the implemented channel code are different for each navigation signal.

This paper is not going to present a detailed description of the data message structure of both signals since the complete specifications can be found in the documents [1][8] and [2]. Nevertheless, some general characteristics of the messages are given:

- **GPS L1C:** Figure 1 shows the GPS L1C frame structure
  - Frame period = 18s
  - Subframe 2 (ephemeris data) → Size = 600 information bits
  - Channel Code over subframe 2: LDPC
    - Channel Code Rate: r = 1/2
    - Systematic: The information bits are not modified
  - Block Interleaver size (symbols): Applied on subframes 2 and 3 ➔ 38 rows and 46 columns

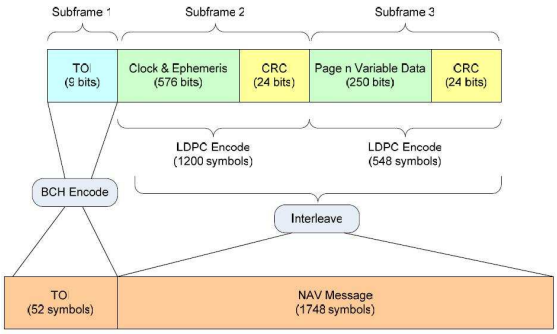


Figure 1: GPS L1C frame structure

- **GALILEO E1 OS:** Figure 2 and 3 show the subframe and page part structure of this message
  - Subframe period = 30s
  - Pages 1 to 4 → Contain the ephemeris and clock corrections
  - Page duration = 2s; Page size = 240 information bits; Each page is constituted by 2 page parts (odd and even)
  - Page part period = 1s; Page part size = 120 information bits
  - Channel Code over a page: Convolutional Code
    - Chanel Code Rate: r = 1/2
    - G1 = 171o; G2 = 133o
    - Non systematic

    → Each page contains 6 tail bits meaning that the convolution code is used as a block code: the size is fixed and the initial and final states are known.
  - Block Interleaver size (symbols): Applied on a page part ➔ 30 rows and 8 columns

T_0 (GST$_0$ sync.) (s)	E1-B Content	E1-B Page	E1B Sub frame ID
0	Spare Page (2/2) | Res. | SAR | Spare | CRC | Res.	Odd	N-1
1	Page 2 (1/2)	Even	N
2	Page 2 (2/2) | Res. | SAR | Spare | CRC | Res.	Odd	N
3	Page 4 (1/2)	Even	N
4	Page 4 (2/2) | Res. | SAR | Spare | CRC | Res.	Odd	N
5	Page 6 (1/2)	Even	N
6	Page 6 (2/2) | Res. | SAR | Spare | CRC | Res.	Odd	N
7	Page 7 or 9 (1/2)	Even	N
8	Page 7 or 9 (2/2) | Res. | SAR | Spare | CRC | Res.	Odd	N
9	Page 8 or 10 (1/2)	Even	N
10	Page 8 or 10 (2/2) | Res. | SAR | Spare | CRC | Res.	Odd	N
11	Reserved (1/2)	Even	N
12	Res. (2/2) | SAR | Spare | CRC | Res.	Odd	N
13	Reserved (1/2)	Even	N
14	Reserved (2/2) | SAR | Spare | CRC | Res.	Odd	N
15	Reserved (1/2)	Even	N
16	Reserved (2/2) | SAR | Spare | CRC | Res.	Odd	N
17	Reserved (1/2)	Even	N
18	Reserved (2/2) | SAR | Spare | CRC | Res.	Odd	N
19	Reserved (1/2)	Even	N
20	Reserved (2/2) | SAR | Spare | CRC | Res.	Odd	N
21	Page 1 (1/2)	Even	N
22	Page 1 (2/2) | Res. | SAR | Spare | CRC | Res.	Odd	N
23	Page 3 (1/2)	Even	N
24	Page 3 (2/2) | Res. | SAR | Spare | CRC | Res.	Odd	N
25	Page 5 (1/2)	Even	N
26	Page 5 (2/2) | Res. | SAR | Spare | CRC | Res.	Odd	N
27	Spare Page (1/2)	Even	N
28	Spare Page (2/2) | Res. | SAR | Spare | CRC | Res.	Odd	N
29	Spare Page (1/2)	Even	N
30	Spare Page (2/2) | Res. | SAR | Spare | CRC | Res.	Odd	N

Figure 2: GALILEO E1 subframe structure

Page Part 1

Even/odd=0	Page Type	Data j (1/2)	Tail	Total (bits)
1	1	112	6	120

Page Part 2

Even/odd=1	Page Type	Data j (2/2)	Reserved 1	SAR	Spare	CRC_j	Reserved 2	Tail	Total (bits)
1	1	16	40	22	2	24	8	6	120

Figure 3: GALILEO E1 OS page structure

III. MOBILE CHANNEL

In this section the main characteristics of the mobile channel, the different types of mobile channel, the type of mobile channel suiting our needs, and the selected mathematical model [9] are presented.

A. Main characteristics:

There are two main characteristics of the mobile environments:

- The direct or LOS signal can be totally or partially blocked / shadowed during the transmission.
- The LOS signal multipath or echoes power is no longer negligible in front of the LOS signal power.

B. Type of Mobile Channel:

The mathematical model simulated in this paper has been selected depending on the type of mobile channel suiting better the needs of this analysis. In fact, the chosen mathematical model correctly represents the transmission channel when the demodulation performance is searched but should be improved if the code tracking performance is inspected.

Two main parameters can classify the different types of mobile channel, the channel coherence bandwidth, $(\Delta f)_c$, and the channel coherence time, $(\Delta t)_c$. Therefore, before determining the type of channel, these two parameters are defined from the received signal expression.

Being the multipath components or echoes the refractions, reflexions, etc of the transmitted signal arriving at the receiver's antenna by another path different from the direct one, LOS path; these echoes can be modeled as a succession of transmitted signals arriving at different delays. Moreover, due to the variability of the surroundings, the movement of the transmitting satellite and the receiver, the delay and the attenuation of the echoes vary at each instant. Therefore, the received band-pass signal can be expressed as:

$$x(t) = \sum_n \alpha_n(t) s\left[t - \tau_n(t)\right] \quad (1)$$

With:

- x(t): received band-pass signal
- s(t): transmitted signal
- $\alpha_n(t)$: Complex attenuation factor for the n^{th} path
- $\tau_n(t)$: Delay of the n^{th} path

The transmitted signal can be expressed using its equivalent baseband complex envelope expression:

$$s(t) = \mathrm{Re}\left[s_l(t) e^{j2\pi f_c t}\right] \quad (2)$$

With:

- f_c: Carrier frequency of the signal
- $s_l(t)$: Equivalent baseband complex enveloppe

Thus, if we express the equivalent baseband received signal, $r_l(t)$:

$$r_l(t) = \sum_n \alpha_n(t) e^{-j2\pi f_c t \tau_n(t)} s_l\left[t - \tau_n(t)\right] \quad (3)$$

Finally the equivalent baseband channel can be described as, $c(\tau, t)$:

$$c(\tau; t) = \sum_n \alpha_n(t) e^{-j2\pi f_c t \tau_n(t)} \delta\left[\tau - \tau_n(t)\right] \quad (4)$$

Then, from this expression of the channel, the channel coherence bandwidth and the channel coherence time can be defined.

First of all, $(\Delta f)_c$ is the inverse of the multipath spread of the channel, T_m, [4]. T_m is the channel impulse response length or the spanning of the echoes, and thus, it is quantified by the time offset between the LOS signal and the last echo. Figure 4 shows the T_m of a possible received signal:

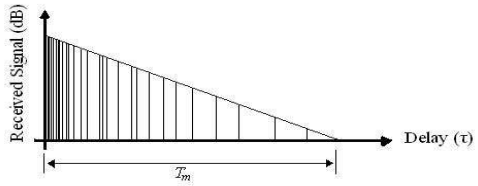


Figure 4: Spanning of the signal echoes channel impulse response - Multipath spread of the channel

Therefore, it can be seen that depending on the symbol or chip duration in relation to T_m, the channel affects differently the signal. In fact, if the symbol or chip duration is much larger than the multipath spread, it can be considered that the received symbol is only affected in amplitude and phase since all the echoes fall mainly on the transmitted LOS symbol duration; however, if the symbol/chip is smaller, the current transmitted symbol affects the to-be-transmitted symbols and thus an intersymbol interference appears, ISI. The reason for the ISI appearance is that the echoes mainly fall outside the transmitted LOS symbol duration.

To sum up, being T the chip duration and W the signal bandwidth with $T \approx 1/W$:

- If $W < (\Delta f)_c$ the channel is frequency non-selective and all the signal is affected equally by the multipath.
- If $W > (\Delta f)_c$ the channel is frequency-selective and the signal is distorted by the multipath.

Concerning the channel coherence time, it can be seen from expression (4), that the delay, attenuation and phase of each received echo vary for each instant of time. More precisely, although the echoes are completely independent among them, they are not uncorrelated to themselves in time. This means that the values of delay, phase and attenuation of the n^{th} echo at time t_1 are related with the same values at time t_2. Therefore, the $(\Delta t)_c$ represents the duration of time in which the channel remains about constant. This variation of the channel is termed *fading*. Therefore, if a symbol or chip duration of a signal increases, the received signal will be more affected by the fading. To sum up:

- If $T < (\Delta t)_c$ the channel is slowly fading and is considered invariant during the symbol duration (T).
- If $T > (\Delta t)_c$ the channel is not slowly fading.

C. Determination of Mobile Channel Type:

In this subsection, the type of mobile channel best suiting the characteristics of the propagation channel from the demodulation performance point of view is determined.

The first characteristic to settle is to determine if the channel is slowly fading. In order to do so, this paper compares the channel coherence time with different symbol/chip durations. We first compute the signal Doppler spread, σ_v, which is the inverse of $(\Delta t)_c$. The Doppler spread power is the addition of three terms [16]:

$$\sigma_v^{\,2} = \left(\frac{V_g}{\Lambda_c}\right)^2 + \left(\frac{\Omega_S}{\alpha_c}\right)^2 + \left(\frac{1}{T_{ch}}\right)^2 \qquad (5)$$

With:

- (V_g/Λ_c): Doppler spread introduced by the mobile motion.
  - V_g = Mobile Speed with respect to the local reference frame.
  - Λ_c = Coherence length which is usually of the order of a signal wavelength (λ).
- (Ω_s/α_c): Doppler spread introduced by the satellite motion
  - Ω_s: Satellite Angular Velocity
  - α_c: Coherence Angle which is determined by the structure of the scenario scatters.
- T_{ch} = Channel self-Doppler Spread

Concerning the Doppler spread introduced by the satellite motion, its typical value for a LEO satellite is about 1Hz [16], and thus, since the Ω_s is smaller for a MEO satellite, this term can be neglected in front of the Doppler spread introduced by the mobile motion. Moreover, T_{ch}, the Doppler spread of the received signal if neither the satellite nor the ground station move, is also marginal in comparison with the Doppler spread caused by the mobile motion [16]. Therefore, the signal Doppler spread can be reduced to only one term:

$$\sigma_v \approx \frac{V_g}{\lambda} \qquad (6)$$

From this expression, it is possible to calculate for a given symbol or chip period the maximum speed at which the mobile should travel if the channel is slowly fading:

$$(\Delta t)_c > T \qquad (6)$$

$$V_g < \frac{c}{T \cdot f_c} \qquad (7)$$

With:

- T: symbol/chip period
- c: speed of light
- f_c: signal frequency carrier

Therefore, giving some examples in table 3:

Symbol/Chip Period	***Max Speed***
20ms	34.3 km/h
10ms	68.6 km/h
4ms	171.38 km/h

Table 3: Maximum allowed speed of a mobile in relation to the symbol/chip period for a slowly fading channel

To sum up, the channel is slowly fading for a mobile travelling at speed of 30km/h even when the symbol/chip period is equal to 20ms. Therefore, from now on, this paper always considers the channel to be slowly fading.

Once this paper has determined that the channel is slowly fading, it has to find out if the channel is frequency-selective or frequency non-selective. Nevertheless, this question no longer matters because, due to the spreading spectrum signal construction and the slowly fading characteristic, both channels, frequency-selective and non-selective, have the same mathematical model from the demodulation performance point of view.

The reason is the following: the mathematical model of a frequency-selective channel is a tapped delay line with tap spacing 1/W and tap weight coefficients $\{c_n(t)\}$ [4] whose distribution is explained later, during the selection of the suiting mathematical model. Moreover, this tapped delay line is truncated at $L = [T_m W] + 1$ for all practical purposes. Figure 5 shows the diagram of such a channel:

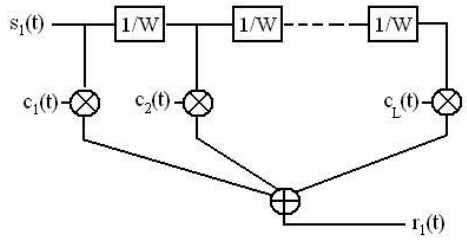


Figure 5: Mathematical model for a frequency-selective channel - A truncated tapped delay line

Where:

$$r_l(t) = \sum_{k=1}^{L} c_k(t) s_l\left(t - \frac{k}{W}\right) \qquad (8)$$

Therefore, at the receiver correlator output:

$$r_l(t) = \sum_{k=1}^{L}\left[c_k(t) s_l\left(t - \frac{k}{W}\right) * c_{PRN\,l}(t)\right] \qquad (9)$$

With:

- $c_{PRNl}(t)$: PRN code of the satellite l

Therefore, since all the echoes are delayed of at least one chip period, their contribution at the prompt correlator output is about 0, which means that at the correlator output the signal is equal to:

$$r_l(t) = c_1(t) s_l\left(t - \frac{k}{W}\right) * c_{PRN\,l}(t) \qquad (10)$$

And this expression is exactly the same one as for a frequency non-selective channel [4] which is illustrated in figure 6:

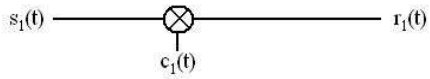


Figure 6: Mathematical model for a frequency non-selective channel

Nevertheless, as has already been said before, this statement is only true when the channel is slowly fading. In fact, if the channel is slowly fading, it is correct to assume that all the correlations between the PRN pilot codes and data codes, as well as the autocorrelations of the codes themselves are ideally orthogonal and triangular. Therefore, none interference is generated. However, in the case where the channel is not slowly fading, all the correlations and autocorrelations of the codes are distorted and thus lose their properties if the received signal phase is not perfectly tracked. The pilot and channel codes are no longer uncorrelated and their autocorrelation is no longer 1 at 0, and 0 outside the chip length. Therefore, a lot of interferences appear and a much more complex and complicated model should be generated to simulate this situation.

To sum up, if the channel is slowly fading, regardless of the channel coherence bandwidth, the frequency non-selective mathematical model can be correctly selected and implemented in the simulator from the point of view of the demodulation performance. However, it would be interesting to analyze the demodulation performance of a frequency-selective channel using the echoes with a Rake Receiver.

D. Mathematical Channel Model:

The mathematical model selected to simulate the transmission channel in a mobile environment, always from the demodulation performance point of view, is the model defined by Perez-Fontan [9].

In fact, Perez-Fontan divides the generation of the transmission channel into 3 different elements depending on the speed with which they influence the resulting signal. These 3 elements are: the very slow variations of the direct signal due to the shadowing or blockage effects, the slow variations of the direct signal due to the different degrees of shadowing of the same obstacle, and the fast variations or fading of the direct signal due to the multipath [9].

In the following subsections the different types of variations, as well as the final mathematical model which groups all of them, are presented.

D-1. LOS very slow variations:

The very slow variations of the LOS signal are produced by different significant shadowing conditions. This means

that the LOS of the mobile to the satellite is blocked by a different type of obstacle, e.g., the LOS is blocked by a building, or by a tree or by nothing at all.

These slow variations are different significant attenuations suffered by the LOS signal and are represented by the selected mathematical model as different states. In the Perez-Fontan model [9], the number of states is equal to 3 and they are named as:

- S1: LOS conditions
- S2: Moderate shadowing conditions
- S3: Deep shadowing conditions.

The transitions between them are modeled as a first-order Markov chain where the mobile remains into the same state for a period equal to the time required by the mobile to cross the state length (L_{Frame}). When the state length has been crossed, the state transition probabilities are used to determine whether the mobile changes of state or remains into the same one. The transition probabilities are stored into the State Transitions Probability Matrix, [P], where the element P_{ij} indicates the probability of passing from the state *i* to the *j* one. Figure 7 illustrates the transitions of states:

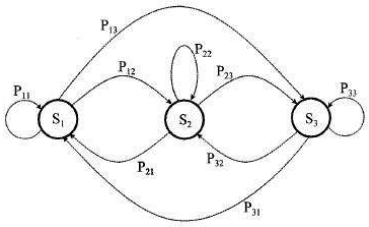


Figure 7: First-order Markov chain for a 3 states model representing the LOS very slow variations

Nevertheless, in this paper, for a first study, only the performance of the signal received in the S1 state is evaluated.

D-2. LOS slow variations:

The slow variations of the LOS signal are produced by small-scale changes in the shadowing attenuation of the same blocking obstacle. In other words, the slow variations are the shadow variations suffered by the LOS signal when the mobile travels in the shadow of the same obstacle. One example is the different leaf and branch densities behind a group of trees.

The slow variations are mathematically represented by a log-normal distribution whose rhythm of variation is determined by the correlation distance (L_{Corr}). In other words, this distance determines the time between new independent samples obtained from the log-normal distribution. Nevertheless, since more samples should be generated between them, an interpolator has to be introduced in order to relate the two independent log-normal samples with the intermediate samples between them.

D-3. Multipath:

The multipath, which has been explained before in the type of mobile channel subsection, is responsible of the fastest variations suffered by the received signal. This effect, as has already been explained, is called fading.

The mathematical model representing this multipath effect is a complex number whose amplitude follows a Rayleigh distribution and whose phase follows a uniform distribution [4]. Therefore, in order to generate these random variables, the most common form of doing so is to generate two Gaussian variables, independent with each other, generating the real and the imaginary part of a complex noise. Nevertheless, since the variation between consecutives attenuations and phases is not independent, the generation of these Gaussian variables is done by applying a low-pass filter with a cut-off frequency equal to the Doppler spread. An adequate filter representing the satellite-mobile user communications is the Butterworth filter [11].

$$\left|H_{Butt}(f)\right|^2 = \frac{B}{1+\left(f / f_{c-off}\right)^{2k}} \qquad (11)$$

With:

- B: Constant setting the filter gain to 1
- $f_{c\text{-}off}$: cut-off frequency
- k: filter order

D-4. Loo Distribution:

In the last 2 subsections, we specified the LOS slow variations as well as the multipath, and we described how they can be simulated. However, these two elements can be grouped into one more compact expression: a random variable which follows a Loo distribution [12], a distribution representing a log-normal distribution for the LOS signal and a Rayleigh distribution for the multipath.

$$p(r) = \frac{r}{b_0\sqrt{2\pi d_0}} \int_0^\infty \frac{1}{z} \exp\left[-\frac{(\ln z - \mu)}{2d_0} - \frac{r^2+z^2}{2b_0}\right] \cdot I\left(\frac{rz}{b_0}\right) dz \qquad (12)$$

Where:

- α: log-normal mean (dB)
  - $\alpha = 20\log_{10}\left(e^{\mu}\right)$
- Ψ: log-normal standard deviation (dB)
  - $\Psi = 20\log_{10}\left(e^{\sqrt{d_0}}\right)$
- MP: Average Multipath Power (dB) in relation to a 0dB hypothetical LOS signal power
  - $MP = 10\log_{10}\left(2b_0\right)$

Therefore, α, Ψ and MP values define a Loo distribution.

Finally, the tap weight coefficients $\{c_n(t)\}$ of the frequency-selective and frequency non-selective mathematical models are used to introduce this Loo distribution followed by the signal. Note that the $\{c_n(t)\}$ mean power should be decreased for each growing index *n* in order to simulate the statistic power loss due to extra travelled distance by the echo. Obviously, this power reduction is done over the mean value because for instant values, due to the Loo distribution, some echoes with bigger index n can have bigger amplitudes than the LOS signal or some previous echoes.

D-5. Final Mathematical Model:

The final received signal can have 3 different states. In each state, the signal follows a Loo distribution whose parameters are defined individually for each state.

In other words, the simulator represents the LOS very slow variations, the LOS slow variations and the multipath component by means of a signal following a Loo distribution, whose parameters represent the different blockage or shadowing and the fading. The Loo parameters change for each state and satellite elevation angle in order to simulate the entire range of situations of the considered scenario: buildings, trees, etc. Finally, the transition between states depends on the mobile speed, the frame length and the state transition probabilities matrix.

IV. PHASE TRACKING METHODS:

One of the characteristics introduced by the mobile channel is a much faster and more random than usual variation of the received signal phase. Therefore, in this paper, in addition to analyzing how the typical Phase Locked Loop reacts to this new type of channel, another phase tracking method is inspected and its performance quantified: the channel estimation. Three different carrier phase tracking methods are evaluated on this study:

1- Traditional Phase Locked Loop
2- Ideal Pilot Channel estimation
3- Proposed Pilot Channel estimation

A. Traditional Phase Locked Loop:

The PLL implemented in this simulation is the typical PLL whose parameters have been defined by [17]. The PLL is only applied over the pilot channel and has an integration time of 20ms. The equivalent noise bandwidth, B_L, is equal to 10Hz and the filter is of 3rd order. The carrier phase loop discriminator chosen to conduct the simulation is the Q pilot channel correlator output.

Moreover, a phase lock detector has been implemented in order to know when the PLL is no longer capable of tracking the signal and what is the percentage of time where this loss of lock occurs. The phase lock detector model applied was defined in [18].

Finally, the only source of error implemented in the simulation is the thermal noise. Therefore, the dynamic stress error, the vibration induced phase noise and the impact of the oscillator clock Allan deviation phase noise have been neglected. For the dynamic stress error, the hypothesis is justified for a car, since the receiver is fixed at some point of the vehicle and does not suffer sudden movements. For the Allan noise and the vibrations, their impact is marginal in front of the thermal noise at the analyzed C/N0 values [19].

B. Channel estimation:

The objective of the channel estimation phase tracking process is to estimate the phase and the amplitude introduced by the channel and to equalize them in order to maximize the SNR of the signal.

The mathematical expression of the channel estimation is displayed next. Assuming that the signal at the receiver ADC output is:

$$r[k] = c_k \cdot s[k] + n[k] \tag{13}$$

$$c_k = |c_k| \cdot e^{j\theta_k} \tag{14}$$

Where:
- r[k]: received signal
- s[k]: transmitted signal
- c_k: Complex number with amplitude and phase of the equivalent propagation channel impulse response. The phase variation due to the satellite-receiver distance variation is not reproduced here.
- n[k]: Additive Gaussian Noise after RF/IF filtering

Note that this paper assumes that signal was transmitted with a phase equal to zero and that the received signal phase is completely introduced by the channel.

And assuming that the system is capable of well estimating the value c_k introduced by the channel, the estimation is:

$$c_{est_k} = |c_{est_k}| \cdot e^{j\theta_{est_k}} \tag{15}$$

$$c_{est_k} = c_k \rightarrow \begin{cases} |c_{est_k}| = |c_k| \\ \theta_{est_k} = \theta_k \end{cases} \tag{16}$$

The equalization of the channel is done by multiplying the received signal with the conjugate of the estimation [4]:

$$v[k] = \overline{c_{est_k}} \cdot r[k] = \overline{c_{est_k}} \cdot (c_k \cdot s[k] + n[k]) \quad (17)$$

$$v[k] = |c_k|^2 s[k] + \overline{c_{est_k}} \cdot n[k] \quad (18)$$

Obviously, the represented case above is the ideal one, when for each sample the system is able to estimate the true channel equivalent impulse response with no error. However, in reality, the system will divide the time in periods, and will use only the samples of one period to estimate the channel equivalent impulse response of this time period. We call this channel equivalent impulse response estimation of one period of time, channel estimation period. And, depending on the estimation technique implemented, these channel estimation periods can be either a constant value, or an interpolation, or a function, etc. Moreover, each channel estimation period is only applied over the period of time samples used to calculate the estimation channel period. Finally, any channel estimation period is sure to not to be perfect since all the possible estimation techniques are always affected by the AG colored noise present in the channel.

To sum up, this paper will analyze the performance of the ideal channel estimation and the performance of one channel estimation method. And this channel estimation method consists in averaging samples of the received signal over specific periods of time in order to obtain a representative complex value of the attenuation and the phase of the channel equivalent impulse response for each period of time.

Nevertheless, before presenting the actual channel estimation methods, the signal mathematical expression for a GNSS received signal having the pilot and data channel in-phase is presented:

$$r[k] = s_d[k] + s_p[k] + n[k] \quad (19)$$

$$\begin{cases} s_p[k] = c_k \cdot e^{j\theta_k} \cdot c^d[k] \\ s_d[k] = c_k \cdot e^{j\theta_k} \cdot d_m \cdot c^p[k] \end{cases} \quad (20)$$

Where:

- $s_d[k]$: Data channel signal
- $s_p[k]$: Pilot channel signal
- $c^d[k]$: PRN code for the data channel
- $c^p[k]$: PRN code for the pilot channel
- d_m: Symbol m value
- c_k: Complex number with amplitude and phase of the equivalent propagation channel impulse response. The phase variation due to the satellite-receiver distance variation is not reproduced here.
- n[k]: Additive Gaussian Noise after RF/IF filtering

Therefore, in the GNSS signal case, the channel estimation is made over the pilot channel since it is affected exactly in the same manner as the data channel but it is not distorted by the symbol value.

B-1. Ideal pilot channel estimation:

In order to analyze which is the limit or lower bound of performance of the pilot channel estimation, the analysis of the demodulation performance in the ideal channel estimation case has to be studied. Therefore, in this case, this paper is going to assume that the system is able to provide an exact estimation of the amplitude and phase introduced by the channel for each sample of the signal.

B-2. Proposed pilot channel estimation:

The pilot channel estimation technique proposed in this study is probably the simplest and worst technique that exists, therefore the BER, WER and EER obtained could be considered as upper bounds.

The proposed estimation consists in: first, averaging a group of pilot samples in order to obtain an average value representative of the channel period. Second and last, applying the estimation on the data samples which have been collected at the same instant as the pilot samples used to calculate the average. The average calculation is accomplished by:

$$c_{est} = c_{avg} \cdot e^{j\theta_{avg}} = \frac{1}{N} \sum_{n=0}^{N-1} c_n \cdot e^{j\theta_n} \quad (21)$$

Therefore the resulting signal after the equalization is:

$$v[k] = s_d[k] \cdot c_{avg} \cdot e^{-j\theta_{avg}} \quad (22)$$

$$v[k] = d_m \cdot c_k \cdot c_{avg} \cdot e^{j(\theta_k - \theta_{avg})} \cdot c^d[k] + n_d'[k] \quad (23)$$

$$n_d'[k] = n_d[k] \cdot c_{avg} \cdot e^{-j\theta_{avg}} \quad (24)$$

One last remark about the pilot channel estimation is that this estimation has to be done over a period of time within which the channel does not vary. If the channel changes, the estimation introduces a lot of errors due to the significant difference between the estimated values and the true ones. Note that this restriction is equivalent to the imposition of the maximum symbol or bit period for a slowly fading channel. Therefore, for a given mobile speed, the maximum time length used to generate a pilot estimation channel is fixed.

V. ASSUMPTIONS OF THE STUDY:

In this section, the assumptions made by this paper in order to simplify the simulations providing the demodulation performance are presented and justified.

There are 3 main assumptions: the assumption of an ideal code tracking, the absence of the synchro-frame process and the perfect achievement of an acquisition process whenever the PLL has lost its lock. Each of these is discussed below.

A. Seamless code tracking process assumption

In order to simplify the analysis, the contribution of the delay tracking process on the sampled value is removed. In fact, the hypothesis taken by this document is that the DLL has already been applied and has lead to a perfect estimation of the delay value.

This hypothesis is justified because the code tracking threshold is lower than the phase tracking threshold [18], therefore this paper assumes that for the analyzed levels of C/N0, the code tracking is perfect or achieved with a negligible error.

The consequence of this assumption is easily observed on the mathematical expression of the signal. Starting from the noiseless LOS conditions model of the correlator output:

$$r_i(\hat{\tau}+(k+1)T_D) = Ad((k+1)T_D)\cdot R(\tau-\hat{\tau})\cdot\cos(\theta-\hat{\theta}) \qquad (25)$$

Where:

- $r_i(n)$: Sampled signal at the correlator output at time n
- A: Amplitude of the data symbol
- T_D: Duration of the data symbol
- $d(n)$: Bit n of the data message
- τ: Delay introduced by the channel
- θ: Phase introduced by the channel
- $R(x)$: Correlation function of the GPS L1C or GALILEO E1b PRN code.

Therefore, if the delay estimation is accurate enough not to affect the final sampled value, the former expression becomes:

$$\tau \approx \hat{\tau} \qquad (26)$$

$$r_i(\hat{\tau}+(k+1)T_D) = Ad((k+1)T_D) = A\cdot d_{k+1}\cdot\cos\left(\theta-\hat{\theta}\right) \qquad (27)$$

To sum up, if the code tracking is accurate enough, the demodulation process is not affected by it. However, a degraded code tracking increases the decoded data message BER and also the pseudorange measurement. In this paper, we assume ideal code tracking.

B. Seamless synchro-frame process hypothesis

This paper also assumes that the synchro-frame has already been achieved. The synchro-frame process consists in searching the beginning of a page or subframe in the continuous stream of received bits. Therefore, once this first identification has been done, all the information can be recovered since all the fields, pages, frames, etc, are easily located inside the stream of bits (from the demodulation of certain fields).

The main consequence of this assumption is that all the page parts or subframes are recovered and none of them is lost. Therefore, the simulation will not bother on synchronizing the frame since it always knows where to find the beginning of the frame.

Note that this assumption corresponds to the case where the user receiver has already tracked the signal and has already achieved the synchro-frame, then enters into a building or a zone with loss of the direct path (or with an increase of multipath effects) where tracking is still possible and thus where there is no need to search the synchronization again. In other words, the only main change is a decrease of the C/N_0 value since the available signal power is smaller than before entering this new environment.

C. Perfect acquisition process after PLL loss of lock

This paper assumes that whenever the phase lock detector indicates a PLL loss of lock, the receiver immediately begins an acquisition process. This acquisition process is considered to last 1 second, since the reacquisition of the signal is much faster than its initial acquisition: the search range is reduced to the surroundings of the last known phase, delay and Doppler frequency. Moreover, this paper assumes that this reacquisition process is always achieved perfectly.

The main consequence of this assumption is the minimum loss of bits due to the phase tracking error. In fact, a real acquisition process could have some problems or could not be accomplished at all, situation which will lead to a major loss of bits and thus to an increase of the BER.

VI. SIMULATION BLOCK SCHEME

The simulation implemented in order to calculate the BER, WER and EER associated to the channel code of each navigation signal is shown in figure 8. A brief description of the figure is given below:

Raw Data Generator: Creates the message content (dummy information) and generates the CRC-24Q associated to this data. It reproduces the constant parts from the frame n to the frame n+1 if necessary.
Encoder: Applies the LDPC code for GPS L1C and the convolutional code (171,133) for GALILEO E1 OS.
Interleaver: Interleaves the page part or the subframes.
Synchro-symbols: Only implemented for GALILEO E1 OS. Inserts the synchro-symbols for each page part.

Signal Physical Materialization: Converts the binary message (0/1) into a physical one (+1/-1) ready to be transmitted into the channel.
Channel Tx Simulation: Generates the errors introduced by the mobile channel during the signal transmission.
Synchro-Frame: Detection of the beginning.of the frame/page part. This process is always perfectly achieved.
Deinterleaver: Deinterleaves the subframes/ page part.
Decoder: Application of the FEC. The implemented decoding algorithms are [5] for GPS L1C and the Viterbi algorithm [6] [7] for GALILEO E1 OS.
CRC verification: Executes the CRC verification as specified in [1] and [2].
Information Extractor: Extracts the information if the CRC verification succeeds.
BER, WER and EER: Calculates the BER, the WER and the EER of the transmission.

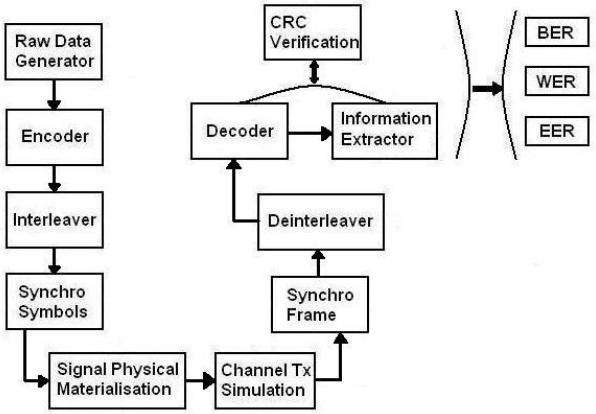


Figure 8: Simulation Block Scheme

VII. SIMULATED CASE

This section presents the simulated case and scenario chosen for this paper in order to obtain a representative demodulation performance, BER, WER and EER, of the GPS L1C and GALILEO E1 OS signals in a mobile environment. Table 4 summarizes the case.

The satellite elevation angle and the mobile speed values have been chosen in order to simulate a representative situation of a car searching position service into a urban environment. Nevertheless, the satellite elevation angle is low and a receiver should normally expect to acquire and to track satellites with a higher angle, but, in this paper, we prefer to present a lower bound of the performance than giving an average or optimistic value.

Moreover, note that the Doppler spread is determined by the mobile speed, derivation of expression (7). Besides, both the PLL integration time and the channel estimation time have been chosen so that the channel is almost constant over these durations: from table 3 we observe that for a symbol duration of 20ms the maximum velocity at which the mobile can travel is about 34 km/h, therefore for a velocity of 30 km/h the channel is constant for 20ms.

Satellite Elevation Angle	30 degrees
Mobile Speed	30 km/h
Doppler Spread	≈ 44 Hz
Simulation State	S1: LOS conditions
Log-Normal Parameters	α = 0.45 dB; ψ = 1.9 dB
Rayleigh Parameters	MP = -16.9 dB
PLL integration Time	20 ms
Channel estimation Time	20 ms

Table 4: Simulated case characteristics

Finally, the simulation only takes place in the LOS conditions state, and the law distribution parameters are taken from the values provided by the DLR in an urban environment for the L-Band [9].

VIII. SIMULATION RESULTS FOR DIFFERENT TRACKING METHODS

The first simulation results illustrated in this paper compare the demodulation performance of the different phase tracking methods presented previously.

In order to conduct this comparison, first the BER and later the EER of the GPS L1C signal are presented for the PLL phase tracking, for the ideal pilot channel estimation and for the proposed pilot channel estimation.

Remember that for all the simulations, the applied conditions have been defined in the section VII and the exact configuration of the PLL has been described in the phase tracking methods section. Moreover, note that the power of GPS L1C and GALILEO E1 OS signals is increased by 0.5 dB due to their transmission through the mobile channel. This gain is expressed by the mean of the log-normal variable. The following figure illustrates the results of the BER comparison:

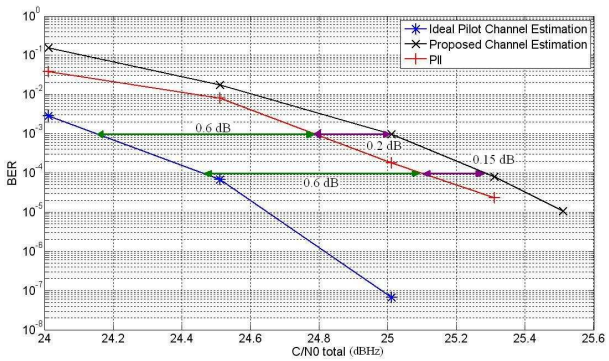


Figure 9: Comparison between ideal pilot channel estimation, proposed pilot channel estimation and PLL tracking method for GPS L1C: BER vs C/N0 (dBHz)

In Figure 9, it can be observed that the difference of performance between the PLL and the proposed estimation method is quite small; about 0.2 dB for a BER equal to 10^{-3}, and a difference of about 0.15dB for a BER equal to 10^{-4}. Moreover, it can be seen that the ideal pilot estimation channel outperforms the results of the PLL, needing 0.6 dB less to obtain a BER equal to 10^{-3} or 10^{-4}. This means that the receiver should have the capacity to obtain the desired level of BER with a lower C/N0 value if a better pilot estimation channel is applied. Nevertheless, it is possible that for this particular case the proposed estimation channel is the best one among the current existing estimation techniques, although it is possible to do better theoretically.

In Figure 9, the simulation of the PLL phase tracking case when the C/N0 is equal to 25.5 dBHz did not have any erroneous demodulated bit. The quantity of transmitted bits was equal to 14200000.

Figure 10 illustrates the same comparison as the figure 9 but with the EER results:

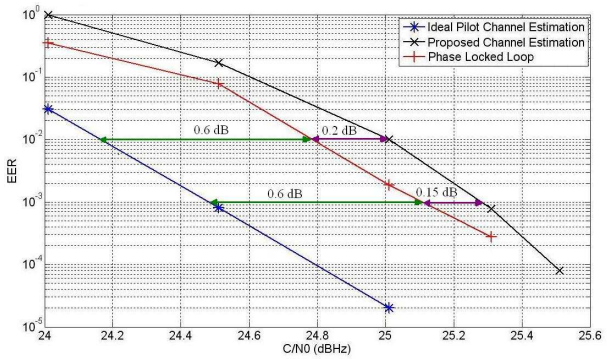


Figure 10: Comparison between ideal pilot channel estimation, proposed pilot channel estimation and PLL tracking method for GPS L1C: EER vs C/N0 (dBHz)

The same observation as for figure 9 can be made. The PLL phase tracking method still outperforms the proposed pilot channel estimation with a gain difference of 0.2 dB for a EER equal to 10^{-2} and 0.15 dB for a EER equal to 10^{-3}. Therefore, the gain differences are the same ones as for the BER, but for EER values being ten times smaller. Moreover, the ideal pilot channel estimation method is still better than the PLL: this fact reinforces the notion of the existence of a real pilot channel estimation method having a better demodulation performance than the PLL demodulation performance.

In this case, the simulation of the PLL phase tracking case when the C/N0 is equal to 25.5 dBHz did not have any erroneous demodulated ephemeris. The quantity of transmitted ephemeris was equal to 24000.

Finally, one last observation is that the PLL has never lost its lock during all the simulations and for all the considered C/N0 values. Therefore, this paper is going to compare the demodulation performance of GPS L1C and GALILEO E1 signals with only the PLL results since this method is the most common phase tracking method applied nowadays.

IX. SIMULATION RESULTS FOR DIFFERENT SIGNALS

In this section the demodulation performance of the GPS L1C and GALILEO E1 OS signals is compared. This comparison is made through simulations calculating the BER, WER and EER of the signals when they are tracked using a PLL.

Moreover, in addition to displaying the curves representing the different GNSS signals BER, WER and EER as a function of C/N0 at the antenna output for their transmission into a mobile channel, the figures also illustrate the performance of these signals for an AWGN channel when a perfect tracking is achieved. The results for an AWGN channel have been taken from [13]. However, since the results of [13] are expressed as a function of the $E_b/N0$, in order to relate the BER, WER and EER values as a function of the C/N0, 23 dBHz have to be added to the GPS L1C $E_b/N0$ values and 24 dBHz to the GALILEO E1 OS ones as has been specified in the reference. However, since the mobile channel adds an average power of 0.5 dB, mean of the log-normal variable, in order to have a fair comparison of the degradation introduced by the noise and the mobile channel in relation to the results of the AWGN channel with ideal tracking, the C/N0 values of this latter channel have been decreased by an offset of 0.5 dB. This means an addition of 22.5 dBHz to the $E_b/N0$ for GPS L1C and 23.5 dBHz for GALILEO E1 OS.

The simulated mobile channel case or scenario as well as the PLL configuration have been explained in previous sections.
The following figure illustrates the results of the BER comparison:

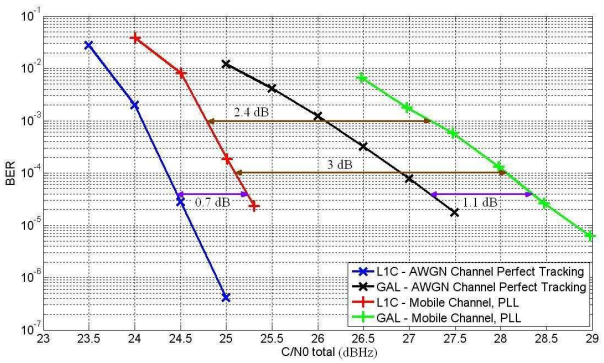


Figure 11: Comparison between GPS L1C and GALILEO E1 OS - BER vs C/N0 total (dBHz) for a mobile channel with PLL tracking

The first observation from the figure 11 is that GPS L1C outperforms GALILEO E1 OS in terms of BER into a mobile channel scenario. More specifically, there is a gain difference favorable to GPS L1C of 2.4 dB for a BER equal to 10^{-3} and 3 dB for 10^{-4}. Moreover, it can be observed that this difference grows with increasing C/N0 values since the slope of the GPS L1C curve is steeper than the GALILEO E1 OS curve. Note that the slope of the curves is determined by the channel code implemented in each signal. Moreover, apart from the slope, the channel code also plays a part into the determination of the absolute values of the curves.

Nevertheless, this outcome was expected since GPS L1C already had better BER results in an AWGN channel. Moreover, it can be observed that, since the tracking process was considered perfect for the AWGN channel simulations, the degradation introduced by the channel and the noise is different for both signals. In fact, this degradation between channels is worse for GALILEO E1 OS than for GPS L1C: whereas for GPS 0.7 additional dB are generally required to obtain the same BER levels between the mobile channel and the AWGN channel, for GALILEO 1.1 dB are normally needed.

However, a priori, this degradation should be expected to be worse for GPS L1C. The reasons are that, despite the fact that GPS L1C provides more percentage of the total amount of power to the pilot channel, the final absolute C/N0 value provided by the system for tracking the pilot channel through a PLL is lower for the GPS L1C than for GALILEO E1 OS when both signals obtain the same BER value. Therefore, the tracking performance of the noisy mobile channel is worse for GPS since the nature of the mobile channel and the nature of the noise are equal for both signals, and thus a worse degradation in terms of demodulation should be expected for GPS. For example, in order to obtain a BER of 10^{-4} for an AWGN channel with a perfect phase tracking process, the GPS L1C receiver needs a total C/N0 of about 24.4 dBHz whereas GALIEO E1 OS needs 26.9 dBHz. This means a pilot channel power of about 23.15Hz for GPS and 23.9 for GALILEO, therefore the tracking performance is worse for GPS.

In fact, this worst tracking performance is shown by the different degradations of the BER between the AWGN channel and the mobile channel suffered by each GNSS signal at a determined total C/N0 value at which both signals obtain the same BER. More specifically, this degradation is represented by a vertical shift of the curve points. For example, into an AWGN noise, for a BER equal to 10^{-4}, GPS needs a C/N0 equal to 24.4 dBHz and GALILEO 26.9 dBHz, whereas, into a mobile channel, GPS L1C obtains for this same C/N0 level a BER bigger than 10^{-2}, and GALILEO E1 OS achieves a smaller value.

Nevertheless, if we want to determine the C/N0 for a 10^{-4} BER value, the additional C/N0 required by GPS L1C is much smaller than the additional C/N0 of GALILEO because the slope of the curves is much steeper for GPS L1C. That slope depends on the signal channel code as it was said before. Moreover, each time the total C/N0 is incremented in order to rise the data channel C/N0 and decrease the BER, the pilot channel C/N0 is also increased; this means that since GALILEO E1 OS needs a bigger amount of C/N0 in order to return to the 10^{-4} BER value, its tracking performance will still improve in relation to the GPS one.

To sum up, although having a bigger C/N0 value to better track the mobile channel and the noise, GALILEO E1 OS suffers a worse degradation than GPS L1C in terms of C/N0 for a determined BER value. The reasons are the GPS L1C channel code and the higher percentage of total amount of power distributed to the pilot channel for GPS.

Figure 12 illustrates the same comparison as the figure 11 but with the WER results:

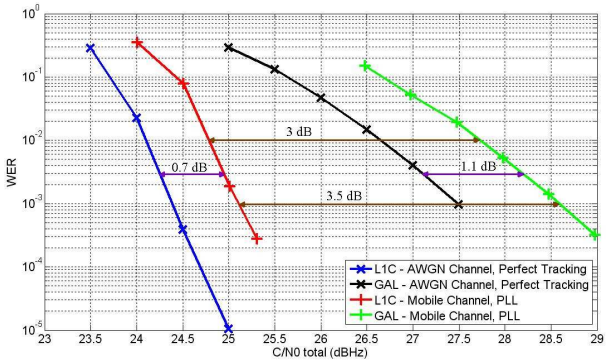


Figure 12: Comparison between GPS L1C and GALILEO E1 OS - WER vs C/N0 total (dBHz) for a mobile channel with PLL tracking

From this figure 12, the same conclusions as for the BER can be extracted. GPS L1C outperforms GALILEO E1 OS in terms of WER as a function of the C/N0 at the receiver antenna output for this mobile channel. For a WER of 10^{-2} there is a difference of 3 dB and for 10^{-3} of 3.5 dB. The same degradation effect is also observed and its reason is the same as before.

The last figure, figure 13, illustrates the results of the EER comparison. In this figure, it can be observed that the gain difference between the signal GPS L1C and GALILEO E1 OS is equal to 3.6 dB for an EER equal to 10^{-2} and 4.1 dB for an EER equal to 10^{-3}.

Moreover, this figure confirms all the observations made in the previous graphics: first, GPS L1C outperforms GALILEO E1 OS in terms of EER as a function of the C/N0 at the antenna receiver output for this mobile scenario. Second, the degradation of demodulation performance introduced by the noise and the mobile

channel in relation to an AWGN channel with perfect tracking is worse for GALILEO E1 OS.

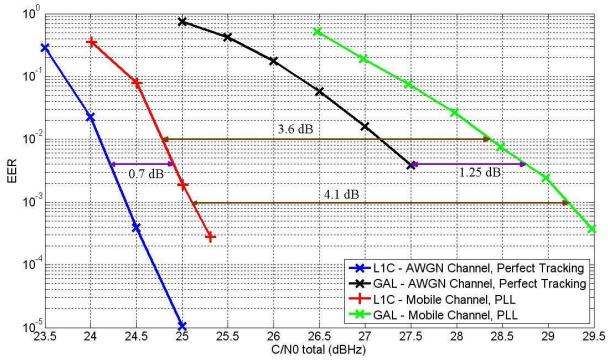


Figure 13: Comparison between GPS L1C and GALILEO E1 OS - EER vs C/N0 total (dBHz) for a mobile channel with PLL tracking

Finally, the following tables summarize the gain difference in terms of C/N0 (dBHz) between the two GNSS navigation signals for the demodulation performance:

Signal	*Canal*	*BER*	
		10^{-3}	10^{-4}
GPS L1C	**Mobile**	24.8	25.1
GALILEO E1 OS	**Mobile**	27.2	28.1
GPS L1C	**AWGN**	24.1	24.4
GALILEO E1 OS	**AWGN**	26.1	26.9

Table 5: BER as a function of the total C/N0 (dBHz) for GPS L1C and GALILEO E1 OS in a mobile and an AWGN channel.

Signal	*Canal*	*WER*	
		10^{-2}	10^{-3}
GPS L1C	**Mobile**	24.75	25.1
GALILEO E1 OS	**Mobile**	27.75	28.6
GPS L1C	**AWGN**	24.1	24.4
GALILEO E1 OS	**AWGN**	26.6	27.5

Table 6: WER as a function of the total C/N0 (dBHz) for GPS L1C and GALILEO E1 OS in a mobile and an AWGN channel.

Signal	*Canal*	*EER*	
		10^{-2}	10^{-3}
GPS L1C	**Mobile**	24.75	25.1
GALILEO E1 OS	**Mobile**	28.35	29.2
GPS L1C	**AWGN**	24.1	24.4
GALILEO E1 OS	**AWGN**	27.1	27.9

Table 7: EER as a function of the total C/N0 (dBHz) for GPS L1C and GALILEO E1 OS in a mobile and an AWGN channel.

Note that all the AWGN channel values should be increased by 0.5 dB since they have been decreased by this exact quantity in order to make a fairer comparison to the mobile channel values since this channel increases in 0.5 dB the power of any signal transmitted through.

Moreover, the C/N0 value for the GALILEO E1 OS signal at an EER equal to 10^{-3} is not displayed on figure 13 but can be obtained from [13].

X. CONCLUSIONS

This paper has analyzed the demodulation performance of different GNSS signals, GPS L1C and GALILEO E1 OS, in a mobile environment with a low satellite elevation angle, 30 degrees. This means that the performance obtained is rather a lower bound since in most cases the tracked satellite will have a higher elevation angle and thus the received signal will be less influenced by the multipath component.

The simulations have shown that GPS L1C outperforms GALILEO E1 OS in terms of BER, WER and EER by a gain difference in terms of C/N0. For example, in order to obtain an EER equal to 10^{-3}, GPS L1C needs about 4.1 dB less than GALILEO E1 OS.

Moreover, through the comparison between the demodulation results for an AWGN channel with perfect tracking and the results for the chosen mobile scenario, it can be concluded the following. For the transmission in the mobile channel, GPS L1C signal needs to add a smaller quantity of dB to the C/N0 values of the AWGN channel than GALILEO E1 OS does, in order to obtain the same BER, WER or EER values for both channels, the mobile channel and the AWGN channel. The main reasons are mainly the different channel code implemented for each signal and the different distribution of power between the pilot and data channel.

Besides, different tracking methods have been analyzed for this particular scenario, resulting in a better performance for the PLL tracking method in comparison to the proposed pilot channel estimation technique performance. More specifically, the PLL requires about 0.2 dB less in terms of C/N0 than the proposed channel estimation method in order to obtain the same BER and EER values. The proposed pilot estimation method is the averaging of the pilot samples and this method can probably be considered as the simplest estimation method. Finally, the ideal pilot estimation method outperforms the PLL in about 0.6 dB in terms of C/N0. Therefore, theoretically, there is or there could be a pilot channel estimation method which provides a better performance than the PLL phase tracking technique.

XI. ACKNOWLEDGMETS

A.G.P. thanks to CNES for the financing of the research fellowship.

XII. REFERENCES

[1] NAVSTAR GLOBAL POSITIONING SYSTEM, *Navstar GPS space Segment/User segment L1C*

interfaces, *Draft IS-GPS-800*, Aug 04, 2006 http://www.losangeles.af.mil/shared/media/document/AF-070803-064.pdf.

[2] *Galileo OS SIS ICD Draft 1*, February 2008. http://www.gsa.europa.eu/go/galileo/os-sis-icd

[3] P. A. Dafesh, E. L. Vallés J. Hsu and D. J. Sklar, L. F. Zapanta, C. R. Cahn, *Data Message Performance for the future L1C GPS Signal*, ION GNSS 20th International Technical Meeting of the Satellite Division, 25-28, September 2007, Fort Worth, TX

[4] John G. Proakis, *Digital Communications*, McGraw-Hill, 2000

[5] David J.C. MacKay, Radford M. Neal, *Near Shannon Limit Performance of Low Density Parity Check Codes*, 12 July 1996, Electronic Letters

[6] A. J. Viterbi, *Error Bounds for Convolutional Codes and an Asymptotically Optimum Decoding Algorithm*, IEEE Transactions on Information Theory, Vol. IT-13, pp. 260-269, 1967.

[7] A. J. Viterbi and J. K. Omura, *Principles of Digital Communication and Coding*, McGraw-Hill, NY, 1979.

[8] J. W. Betz, M. A. Blanco, C. R. Cahn, P. A. Dafesh, et.al., *Description of the L1C Signal*, Proceedings of ION GNSS, Sept. 2006.

[9] F. Perez-Fontan, M. Vazquez-Castro, C. Enjamio-Cabado, J. Pita-Garcia, E. Kubista, *Statistical Modeling of the LMS Channel*, IEEE Transactions on vehicular technology, Vol. 50, NO. 6, November 2001.

[10] F. Perez-Fontan, M.A. Vazquez-Castro, S. Buonomo, J.P. Poiares-Baptista, B. Arbesser-Rastburg, *S-Band LMS propagation channel behaviour for different environments, degrees of shadowing and elevation angles*, IEEE Transactions on Broadcasting, Vol. 44, No. 1, March 1998.

[11] P. Burzigotti, R. Prieto-Cedeira, A. Bolea-Alamañac, F. Perez-Fontan, I. Sanchez-Lago, *DVB-SH Analysis Using a Multi-State Land Mobile Satellite Channel Model*, Advanced Satellite Mobile Systems, 2008. ASMS 2008. 4th

[12] C. Loo, J. S. Butterworth, *Land Mobile Satellite Channel Measurements and Modeling*, Proceedings of the IEEE, Vol. 86, No. 7, July 1998.

[13] A. Garcia-Pena, C. Macabiau, A-C. Escher, M-L. Boucheret, L. Ries, *Comparison between the Future GPS L1C and GALILEO E1 OS Signals Data Message Performance*, Proceedings of the 2009 International Technical Meeting of the Institute of Navigation, January 26 - 28, 2009.

[14] O. Julien, M. E. Cannon, G. Lachapelle, *Impact of Future GNSS Signals on Carrier-Phase Tracking*, CD-ROM Proceedings of European Navigation Conference, Munich, 19-22 July, 16 pages.

[15] C. J. Hegarty, *Analytical Derivation of Maximum Tolerable In-Band Interference Levels for Aviation Applications of GNSS*, Proceedings of the 9th International Technical Meeting of the Satellite Division of the Institute of Navigation ION GPS 1996, September 17 - 20, 1996.

[16] I. Frigyes, B. G. Molnar, R. Vallet, Z. Herczku and Z. Bodnar, *Doppler spread characteristics of satellite personal communication channels*, International Journal of Satellite Communications, 2001.

[17] S.A. Stephens and J.B. Thomas, *Controlled-Root Formulation for Digital Phase-Locked Loop*, IEEE Transactions on Aerospace and Electronic Systems, Vol. 31, No. 1, January 1995,

[18] A.J. Van Dierendonck, *Global Positioning System: Theory and Applications Volume I, Chapter VIII-GPS Receivers*, Volume 163, Progress in Astronautics and Aeronautics, 1996.

[19] O. Julien, *GNSS Solutions Tutorial - CN433 Receiver Signal Processing for Future GNSS Signals – Introduction*, ION GNSS 2009.